

Anatoliy KULIK, Kostiantyn DERGACHOV, Sergiy PASICHNIK, Dmytro SOKOL

National Aerospace University “Kharkiv Aviation Institute”, Kharkiv, Ukraine

RATIONAL CONTROL OF THE TEMPERATURE OF VORTEX ENERGY SEPARATOR UNDER DESTABILIZING INFLUENCE

The **object** of study in this article is the formation process of a rational control of the temperature of a vortex energy separator under destabilizing influences. The **subject matter** of the article is the process of forming a dichotomous tree by two-digit predicates from diagnostic models a vortex energy-separator device as a rational control object when destabilizing influences appear, and its further recovery. The **goal** is to develop an analytical approach to the formation of digital algorithms for the rational control of cold and hot air flow temperatures of a vortex energy separator. The **tasks** are to study the features of the process in the vortex energy-separator device; to describe a rational control system of the vortex energy-separator device; to analyze the experimental characteristics of the vortex energy-separator device; to form linear mathematical models of the nominal mode of the vortex energy-separator device; to develop linear diagnostic models that describe the inoperable states of the vortex energy separator as a rational control object; to form logical signs of diagnosing using diagnostic models, to develop recovering algorithms for the vortex energy separator. The **methods** used are transfer functions, discrete state space, forming production rules, two-digit predicate equations, dichotomous trees, diagnosing and recovering the operability of dynamic objects. The following **results** were obtained: the vortex energy-separation process features analysis, the rational control system structure and function description, the experimental characteristics analysis, the development of mathematical models, diagnostic and recovering tool development for the emergency operation process of a vortex energy separator as a rational control object for a given destabilizing influence set. **Conclusions.** Scientific novelty is the development of an analytical approach to the development of rational control of the vortex separation process of the air flow under the significant influence of various kinds of destabilizing influences.

Keywords: Ranque-Hilsch vortex tube; vortex energy separator; rational control; destabilizing influences; linear mathematical models; predicate equations; diagnostic tool; recovering tool.

Introduction

Intensive technology development significantly affects environment. It is possible to reduce negative impact on biosphere within the energy area not only with saving energy, but also with increasing the purity of ecological technologies. One of such technologies is associated with a vortex effect based on the energy separation of gases. Devices realizing this effect are called vortex energy separators (VES).

At present, VES plays a significant role in industry. This device is one of the non-conventional type refrigerating systems for the production of refrigeration that is used to simultaneously perform cold and hot flows of compressed gas. Due to its compact size, low cost of manufacture, ease of maintenance and repair, no need for refrigerants, high speed of reaching the operating mode, environmental friendliness, the absence of moving parts and simplicity of integration into many systems, VES is able to perform a variety of tasks: cooling, heating, pressure reduction, gas purification, etc. A safety usage of such sensitive objects is quite important, when they directly affect human health.

1. State-of-the-art and Objectives

VES is a technical device that uses the effect of temperature separation in a rotating gas flow, in other words, the vortex effect [1].

Energy transfer in compressible continuous swirling media was discovered by researchers at the beginning of the last century by the French engineer Joseph Ranque while the cyclones operation studying. At the end of 1931, he applied for an invented device, which he called a vortex tube, and only in 1934 he received a patent. In the forties, as a result of research on improving the efficiency of the thermal separation of gases, the German physicist Robert Hilsch obtained new experimental results. In honor of these outstanding researchers, the vortex effect began to be called the Ranque-Hilsch effect, and the device that reproduces this effect was called the Ranque-Hilsch tube. Since the discovery of vortex effect, its intensive study begins with the aim of technical implementation in various technologies [2].

A VES shown in Figure 1, in fact, is a gas-dynamic generator of cold T_c and hot T_h air, using the

potential energy of pre-compressed gas with temperature T_{in} . The thermal energy is converted through the effect of temperature separation in a rotating gas flow.

The operating principle of VES is described in paper [3]. Compressed gas with temperature T_{in} enters the inlet of the nozzle device 1, which is a smoothly tapering channel of rectangular cross section, in which the gas flow is given rotational motion due to the spiral shape of the surface 2. The most common form of the spiral is the Archimedes spiral, which provides the smoothest change in the direction of the velocity vector. The swirling gas flow enters the energy separation chamber 3, moving along a helical trajectory in the near-wall region to the straightening crosspiece 4 and then to the cone valve 5. Passing through the crosspiece, the flow loses the circumferential velocity component, as a result of which the pressure slightly increases. The flow area of the cone valve is not sufficient to pass the entire mass of gas, so part of the flow begins to move in the opposite direction from the valve in the axial region of the energy separation chamber and is discharged through the diaphragm 6.

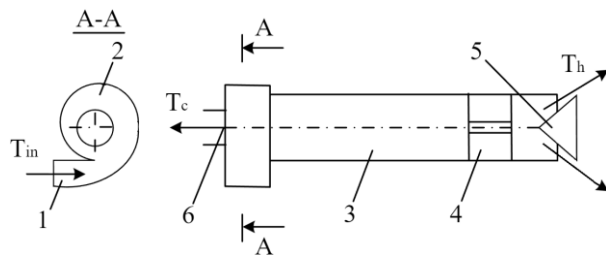


Fig. 1. Scheme of the device of VES:

1 – nozzle device; 2 – twisting device;

3 – energy separation chamber;

4 – crosspiece; 5 – cone valve; 6 – diaphragm

Energy is exchanged due to interaction of counter-moving vortex flows so the peripheral layers are heated and the paraxial ones are cooled. Thus, the temperature of the gas that left the energy separation chamber through the cone valve (T_h) is higher than the temperature of the gas supplied to the VES. Accordingly, the flow exiting through the diaphragm of the gas (T_c) has a lower temperature than the gas at the inlet of VES (T_{in}).

The processes occurring in the VES both in steady state and transient modes are characterized by the following features [4]:

- peripheral flow is a large-scale vortex structure with developed turbulence and moving according to the law of a free vortex;
- paraxial flow has a small-scale turbulent structure and moves in the energy separation chamber according to the forced vortex law;

- vortex flows thermodynamic and kinematic parameters distribution in the volume of the chamber is significantly uneven;

- VES mode parameters are sensitive to changes in both internal and external operating conditions;

- VES parameters significantly depend on the design features and operating conditions of the VES.

The listed features of the temperature separation effect, as well as the insufficient knowledge of nature of this phenomenon, do not allow forming analytically a VES mathematical model as ACO.

The significant non-linearity of the VES static characteristics, the distribution of parameters and their non-stationarity in steady and transient conditions make reasonable usage of adaptive control for vortex gas flow state in order to provide the performance indicators required for various technical applications.

In general, the absence of general analytical regularities describing the processes in VES of various designs leads to the needs of mathematical models forming for specific VES as a result of processing their experimental characteristics. For this purpose, an experimental study of the static and dynamic characteristics was carried out on a mock-up prototype of VES, which has the following geometric characteristics: diameter of the working part D_{wp} is 5.8 mm; length of the working part $L_{wp} = 20 \cdot D_{wp}$; control valve position range $\Delta\mu_{wp}$ is 2 mm; diaphragm diameter D_d is 2.5 mm. External conditions are the compressed air pressure P is from 0.5 to 0.7 MPa and ambient temperature T is 292 K [5].

The paper [6] is about getting the static characteristics of VES based on CFD experimental data. A set of input data as both compressed air parameters and control valve position affects the temperature of output flows. Obtaining the mathematical model requires to enhance such nomograms to be more effective, so the main difference here is to get output-input signals ratio:

- replace cold mass friction with control valve position as the input signal;

- replace temperature drop with the actual value of the temperature itself.

As a result of the experimental study, VES static characteristics as ACO were obtained, reflecting the dependence of the temperature of the cold θ_1 and hot θ_2 air flows on the valve movement for three values of compressed air pressure. These dependences are shown in Figure 2 and Figure 3 respectively.

In order to determine the structure and parameters of the VES transfer functions, its experimental logarithmic amplitude-frequency characteristics (Figure 4 and Figure 5) were obtained for two values of the operation points: μ_{10} is 0.5 mm and μ_{20} is 1.25 mm, as well as for compressed air pressure 0.6 MPa and 0.7 MPa.

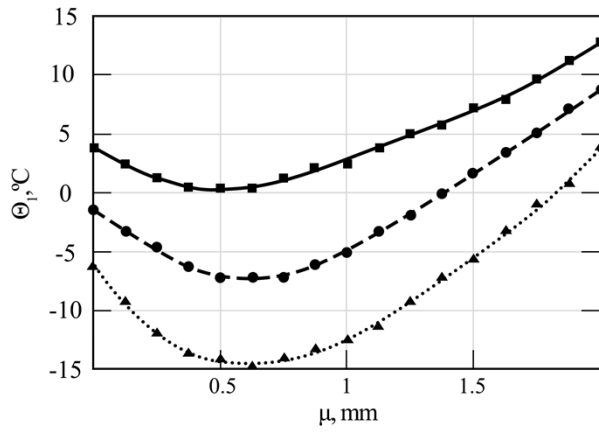


Fig. 2. Graphs of the static characteristics of VES for cold air flow:
 ■ – 0.5 MPa, ● – 0.6 MPa, ▲ – 0.7 MPa

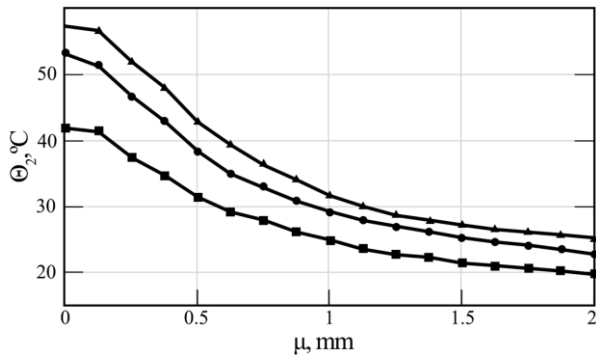


Fig. 3. Graphs of the static characteristics of VES for hot air flow:
 ■ – 0.5 MPa, ● – 0.6 MPa, ▲ – 0.7 MPa

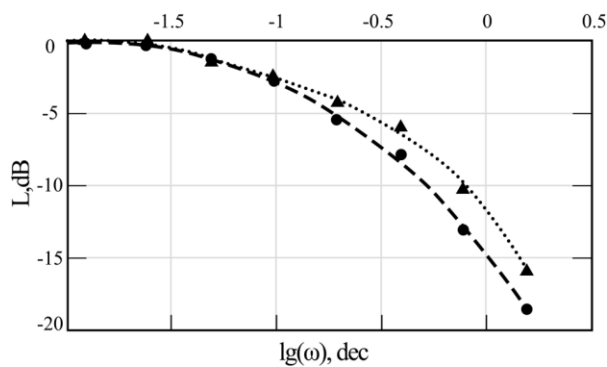


Fig. 4. Graphs of experimental logarithmic amplitude-frequency characteristics of VES for operation point $\mu_{10} = 0.5$ mm:
 ● – 0.6 MPa, ▲ – 0.7 MPa

In order to evaluate the inertial properties and quality indicators of the VES, transient characteristics were experimentally obtained for two values of the operation points μ_{10} is 0.5 mm and μ_{20} is 1.25 mm for pressures 0.6 MPa and 0.7 MPa. (Figures 6 – 9).

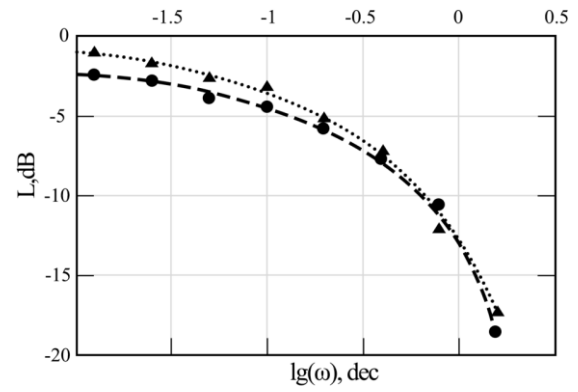


Fig. 5. Graphs of experimental logarithmic amplitude-frequency characteristics of VES for operation point $\mu_{20} = 1.25$ mm:
 ● – 0.6 MPa, ▲ – 0.7 MPa

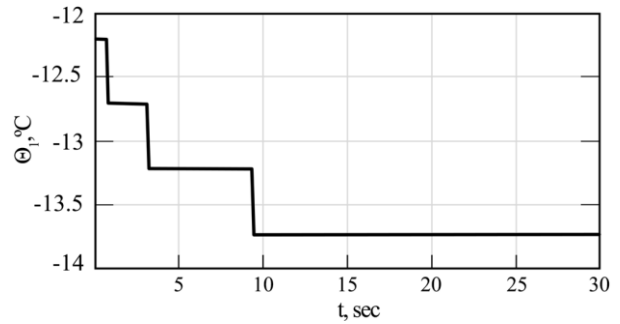


Fig. 6. Transient characteristics of VES for cold air flow when $\mu_{10} = 0.5$ mm

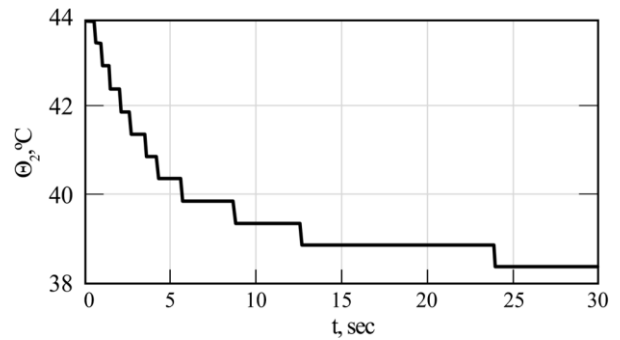


Fig. 7. Transient characteristics of VES for hot air flow when $\mu_{10} = 0.5$ mm

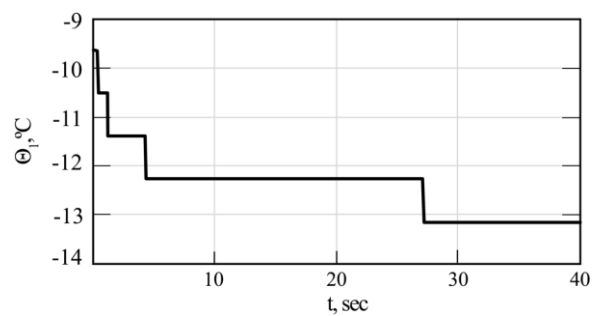


Fig. 8. Transient characteristics of VES for cold air flow when $\mu_{20} = 1.25$ mm

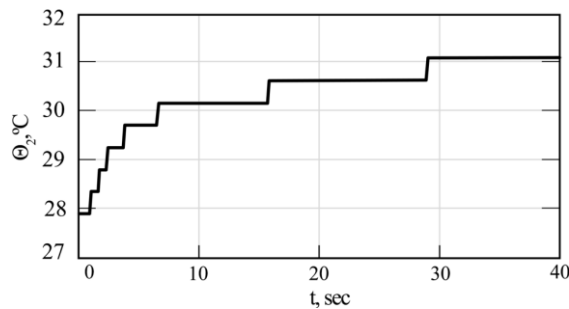


Fig. 9. Transient characteristics of VES for hot air flow when $\mu_{20} = 1.25$ mm

As a result of processing the experimental data of the VES prototype, adequate mathematical models were obtained in the linear approximation for both the cold and hot air flows depending on the valve displacement [5].

Thus, it was found that the energy separation transformation processes in the VES prototype can be approximated for different operation points and at different values of compressed air pressure by first-order linear mathematical models both in the form of differential equations and in the form of transfer functions.

Talking about application of VES in different control systems, several examples are analyzed below, on the basis of which the objectives are formulated.

The paper [7] proposes to use the Ranque-Hilsch vortex tube in the vehicle air conditioning systems. The usage areas of such air conditioning system can be both the car interior and the aircraft cockpit. The disadvantage of the described system is a temperature control in the open-loop system without using information about its output signal. This approach involves the regulation of the required temperature only by directly adjusting control signal, excluding automatic temperature control.

The paper [8] describes an autonomous cooling system, which operates due to the Ranque-Hilsch vortex tube for a vaccine container. The main purpose of that cooling system is to maintain the desired temperature in the refrigerator compartment with minimal temperature fluctuations. Thus, the temperature stabilization within the optimal range of vaccine storage conditions is important rather than its continuous regulation. The fundamental disadvantages of the proposed system are its inability to quickly respond to temperature changes and fend off external destabilizing factors. That is, if the temperature regime deviates from the norm for a long time, external human (staff) intervention in the system operation is required. A similar approach can also be applied for local cooling of on-board aircraft equipment, or parts and machine tools in automatic manufacturing; in these cases, autonomous maintenance of critical temperatures is also required.

One of the main goals of the article [9] is performance increase of the solar thermoelectric generator via the Ranque-Hilsch vortex tube for hybrid vehicles. The paper considers the car, the body of which is covered with solar thermoelectric generator modules, and equipped with a turbogenerator. The energy accumulated by the solar thermoelectric generator modules can be used for the full operation of the vehicle, so the proposed approach can be applied to many unmanned vehicles (land, flying). Following the idea of the article on increasing the efficiency of the solar thermoelectric generator, many parameters of vortex tube outlet flows play an important role. As the authors note, those parameters are changeable in unsteady and non-permanent conditions, in particular, due to the car speed. Thus, automatic tuning and adjustment of the vortex tube parameters are necessary to avoid system performance decrease, which cannot be carried out due to the proposed open-loop system.

Under the similar trend in the Ranque-Hilsch vortex tube application is considered in [10]. A way to increase renewable energy penetration in isolated communities through trigenerative compressed air energy storage systems is being inspected. In order to avoid throttling losses, vortex tubes are proposed to convert part of the excess pressure into useful heating and cooling. As a result, the most optimal configuration of such system is determined, which has a complex design, including the cascade connection of two vortex tubes. The authors also note a possible change in vortex tube characteristics that will inevitably lead to a decrease of the high-potential heat usage in the thermal energy storage. Therefore, maintaining the operability of such complex system at a high level of its performance is the main objective. As a development of the study, the authors propose to improve the system configuration, consider air as a mixture of real gases, and develop more efficient vortex tube. All of these goals are aimed at operating with efficiency, but none of the above significantly increases the system reliability. The question remains of the inability to compensate and fend off both external destabilizing effects on the system and its internal failures.

In the paper [11], vortex tubes are installed on the helicopter engine intakes to remove potentially harmful dust from the influent air to eliminate the risk of rapid engine wear and subsequent power deterioration. The study, that was conducted on the number and axial angle of inlet nozzles to evaluate their impact on general performance, is limited by the fixed parameters of environment in which the helicopter engine is operated. Such significant parameters for the set goals as pollution, pressure, air density directly affect the vortex tube efficiency and are not constant. Then it is necessary to

continuously automatically adjust the system to the current environmental data.

The identified shortcomings of the VES usage significantly reduce the quality indicators of its functioning. High quality control of VES under destabilizing effects can be achieved using a rational control that combines the benefits of intelligent, predictive and adaptive controls [12]. This principle is based on identifying the causes of the failure of VES as an automatic control object (ACO) and restoring its normal functioning. To form a diagnosis, mathematical models that describe both nominal and destabilized modes of functioning are used.

In this paper, a rational control is considered to take into account the following disadvantages of open-loop systems:

- continuous adjustment and adaptation of the control action to system parameter changes via the control closed loop;
- parrying the removable causes of destabilizing factors, and not just compensating for their consequences;
- localization of undesirable impact on the system and rapid response without reference to the transient time of a automatic control system (ACS);
- adjustment of the parameters of the system functioning in order to stabilize the value within the reliable performance of system.

In order to maintain safe operation and acceptable performance of the VES in order to avoid the occurrence of malfunctions, the system should individually respond to uncertainties and disturbances.

Thus, rational control of the VES is carried out, as the most vulnerable and unprotected, at the same time, the main part of ACS, subject to destabilizing influences of an indefinite type.

The article presents the findings of the analytical approach formation to the rational control of VES under single destabilizing effects. The most appropriate for the task at hand is the use of two-stage development of RCS.

2. Rational control method

Rational control is one of the approaches for adaptive control of objects with uncertainty. Destabilizing influences are various uncontrolled disturbing influences, noise, interference, defects, malfunctions and failures that could be considered as uncertain events. The uncertainty of destabilizing influences contains the moment of destabilization occurrence, the functional element that is affected, the type of destabilization which it belongs to, as well as its unknown specific value. A set of destabilizing influences has a finite number.

The elements of that set are specific physical kinds of destabilizations [13].

VES during its operation is subject to a number of destabilizing effects: fluctuations in ambient temperature, changes in compressed air pressure, noise in temperature measurement channels, malfunctions, breakdowns and failures, etc. Destabilizing effects are uncontrolled influences that disrupt the operability of VES and lead to a significant change in the temperature of cold and hot air flows. The use of classical control principles (open-loop and closed-loop systems) does not allow to fully fend off the destabilizing influences and ensure high-quality control of the temperature of the output air flows. Rational control enables to identify the causes of destabilization and fend off them with appropriate tools. Rational control provides a number of specific advantages over each control techniques [14]:

- rapid response;
- feedback controller;
- reliability and survivability resource growth, the operability of the object due to the selective fend off of causes of destabilizing effects;
- diagnosing and neutralizing of destabilizing influences period is less than the transition period of a control action;
- good stability;
- ability to handle any changes that are present in the knowledge base;
- provides attractive features for the situation model parameter uncertainty and external disturbances;
- parameters can be changed fast in response to changes in process dynamics;
- no need to adjust the RCD for the different disturbances, if these influences are in the knowledge base;
- internal parameter variation considers as a parryable disturbance, not a floating model of the plant;
- RCD uses simple logic operations;
- disturbance robustness and shifting in performing conditions, by definition;
- prediction on upcoming disturbance, etc.

Regarding to the problem of automatic control of VES, the rational control system (RCS) consists of two interconnected subsystems. The first subsystem is a rational control object (RCO), the second one is a rational control device (RCD) which are interconnected by signal links. The functional diagram of RCS is shown in Figure 10.

RCO includes a control object, VES, to which compressed air is supplied with pressure P , a servo that changes the cone valve position $\mu(t)$ relative to the energy separation chamber, and temperature sensors for cold $\theta_1(t)$ and hot $\theta_2(t)$ air flows. RCO is affected by a set of uncontrolled destabilizing influences D , i.e., uncertain events.

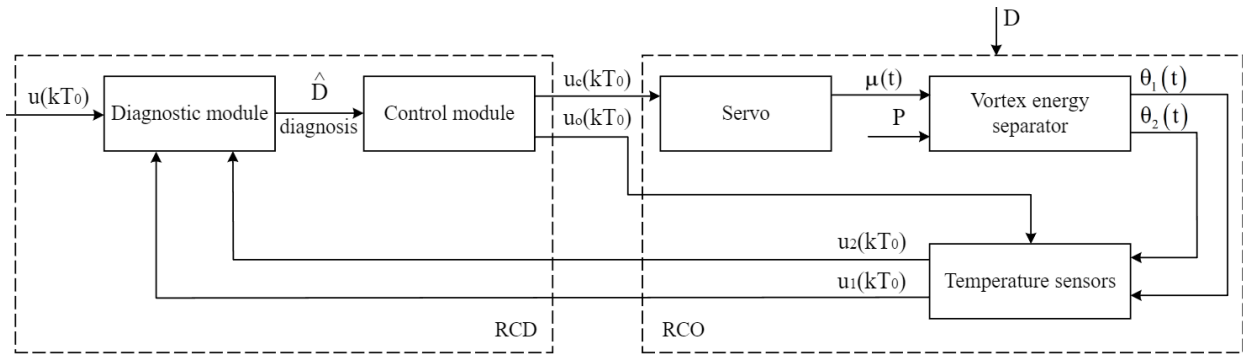


Fig. 10. Functional diagram of RCS

The second subsystem, RCD, consists of diagnostic and control modules. Both modules deal with discrete signals where k is a number of sample and T_0 is a sample time. In the diagnostics module, a functional state diagnosis of RCO is formed as the estimates of destabilizing influences \hat{D} , based on the control signal $u(kT_0)$ and the signals of the temperature sensors $u_1(kT_0)$ and $u_2(kT_0)$. In the control module, control impacts $u_c(kT_0)$ and $u_o(kT_0)$ are formed, recovering the operation of RCO based on the results of its diagnosis.

The diagnostic module is the major part of presented functional diagram. The purpose of this module is to obtain the diagnosis of RCO state. It is required to detect, localize and identify current destabilizing influence via searching the destabilized functional element, determining its type and specific kind.

Detection of a destabilizing influence is the deviation fact establishment in the operation of RCO. Localization consists of the search for the functional element subject to the destabilizing influence. The type is a group of destabilizing influences that lead to the same type of disruption of RCO. The kind of destabilizing influence is its specific physical manifestation, which can be eliminated by means of recovery resources. Thus, diagnostics is performed by the diagnostic module and represents a process of successive removal of uncertainties: to detect the destabilization, to identify the place of its action, to determine its type and kind.

In the presented functional diagram (Figure 10), RCO differs from traditional classical ACO. Together with the necessary properties of, RCO must possess not

only controllability and observability, but diagnosability and recoverability. Diagnosability is the ability to unambiguously define the destabilizing influence due to the signals available for measurement in a finite time. Recoverability is the ability to compensate destabilizing influences due to the hardware and software in a finite time.

Rational control is formed as a result of reasonable combination of analytical tools, computational, mock-up and bench experimental studies, intuition and common sense of developers.

3. Mathematical models of nominal operation mode

The conversion properties of RCO in Figure 10 in the nominal mode, that is, in the absence of destabilizing influences from the set D , can be reflected in a linear approximation using the block diagram shown in Figure 11.

The transfer function of the servo is

$$W_1(s) = \frac{M(s)}{U_c(s)} = \frac{\kappa_1}{s} \tag{1}$$

Transfer functions of VES for cold air flow

$$W_2(s) = \frac{\Theta_1(s)}{M(s)} = \frac{\kappa_2}{T_2s+1} \tag{2}$$

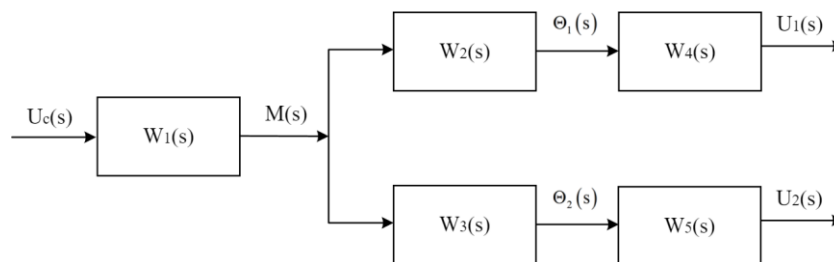


Fig. 11. Block diagram of RCO

and hot air flow

$$W_3(s) = \frac{\Theta_2(s)}{M(s)} = \frac{\kappa_3}{T_3 s + 1}. \quad (3)$$

The transfer functions of the temperature sensors

$$W_4(s) = \frac{U_1(s)}{\Theta_1(s)} = \frac{\kappa_4}{T_4 s + 1}; \quad (4)$$

$$W_5(s) = \frac{U_2(s)}{\Theta_2(s)} = \frac{\kappa_5}{T_5 s + 1}$$

respectively.

Then the transfer function of the cold air flow channel is

$$W_c(s) = \frac{U_1(s)}{U_c(s)} = W_1(s) \cdot W_2(s) \cdot W_4(s) = \quad (5)$$

$$= \frac{\kappa_1 \kappa_2 \kappa_4}{T_2 T_4 s^3 + (T_2 + T_4) s^2 + s}$$

and the transfer function of the hot air flow channel is

$$W_h(s) = \frac{U_2(s)}{U_c(s)} = W_1(s) \cdot W_3(s) \cdot W_5(s) = \quad (6)$$

$$= \frac{\kappa_1 \kappa_3 \kappa_5}{T_3 T_5 s^3 + (T_3 + T_5) s^2 + s}$$

In the state space, the RCO in the nominal mode is described by the following system of equations

$$\begin{bmatrix} \dot{x}_1(t) \\ \dot{x}_2(t) \\ \dot{x}_3(t) \\ \dot{x}_4(t) \\ \dot{x}_5(t) \end{bmatrix} = \begin{bmatrix} 0 & 0 & 0 & 0 & 0 \\ \frac{\kappa_2}{T_2} & -\frac{1}{T_2} & 0 & 0 & 0 \\ 0 & \frac{\kappa_4}{T_4} & -\frac{1}{T_4} & 0 & 0 \\ \frac{\kappa_3}{T_3} & 0 & 0 & -\frac{1}{T_3} & 0 \\ 0 & 0 & 0 & \frac{\kappa_5}{T_5} & -\frac{1}{T_5} \end{bmatrix} \cdot \begin{bmatrix} x_1(t) \\ x_2(t) \\ x_3(t) \\ x_4(t) \\ x_5(t) \end{bmatrix} +$$

$$+ \begin{bmatrix} \kappa_1 \\ 0 \\ 0 \\ 0 \\ 0 \end{bmatrix} \cdot u_c(t); \quad \begin{bmatrix} x_1(0) \\ x_2(0) \\ x_3(0) \\ x_4(0) \\ x_5(0) \end{bmatrix} = \begin{bmatrix} 0 \\ 0 \\ 0 \\ 0 \\ 0 \end{bmatrix};$$

$$\begin{bmatrix} u_1(t) \\ u_2(t) \end{bmatrix} = \begin{bmatrix} 0 & 0 & 1 & 0 & 0 \\ 0 & 0 & 0 & 0 & 1 \end{bmatrix} \cdot \begin{bmatrix} x_1(t) \\ x_2(t) \\ x_3(t) \\ x_4(t) \\ x_5(t) \end{bmatrix}. \quad (7)$$

In order to describe RCO in a discrete state space, one can use the Euler formula, according to which

$$\dot{x}(kT_0) \approx \frac{x[(k+1)T_0] - x(kT_0)}{T_0}, \quad (8)$$

where $k = 0, 1, 2, \dots$ is a sample time, T_0 is a quantization period.

Applying equation (8) to equation (7), the following system of finite difference equations are obtained

$$\begin{bmatrix} x_1[(k+1)T_0] \\ x_2[(k+1)T_0] \\ x_3[(k+1)T_0] \\ x_4[(k+1)T_0] \\ x_5[(k+1)T_0] \end{bmatrix} = \begin{bmatrix} 0 & 0 & 0 & 0 & 0 \\ \frac{\kappa_2 T_0}{T_2} & 1 - \frac{T_0}{T_2} & 0 & 0 & 0 \\ 0 & \frac{\kappa_4 T_0}{T_4} & 1 - \frac{T_0}{T_4} & 0 & 0 \\ \frac{\kappa_3 T_0}{T_3} & 0 & 0 & 1 - \frac{T_0}{T_3} & 0 \\ 0 & 0 & 0 & \frac{\kappa_5 T_0}{T_5} & 1 - \frac{T_0}{T_5} \end{bmatrix} \cdot \begin{bmatrix} x_1(kT_0) \\ x_2(kT_0) \\ x_3(kT_0) \\ x_4(kT_0) \\ x_5(kT_0) \end{bmatrix} +$$

$$\begin{bmatrix} \kappa_1 T_0 \\ 0 \\ 0 \\ 0 \\ 0 \end{bmatrix} \cdot u_c(kT_0); \quad \begin{bmatrix} x_1(0) \\ x_2(0) \\ x_3(0) \\ x_4(0) \\ x_5(0) \end{bmatrix} = \begin{bmatrix} 0 \\ 0 \\ 0 \\ 0 \\ 0 \end{bmatrix};$$

$$\begin{bmatrix} u_1(kT_0) \\ u_2(kT_0) \end{bmatrix} = \begin{bmatrix} 0 & 0 & 1 & 0 & 0 \\ 0 & 0 & 0 & 0 & 1 \end{bmatrix} \cdot \begin{bmatrix} x_1(kT_0) \\ x_2(kT_0) \\ x_3(kT_0) \\ x_4(kT_0) \\ x_5(kT_0) \end{bmatrix}. \quad (9)$$

This system of equations can be represented in a more compact form

$$x(k+1) = A \cdot x(k) + b \cdot u(k); \quad x(0) = x_0; \quad (10)$$

$$u(k) = C \cdot x(k),$$

where $x(k)$ is the state vector, $\dim[x(k)] = 5$, A , b and C are the matrices of the corresponding dimensions, $u(k)$ is the output vector, $\dim[u(k)] = 2$.

In the discrete space of states, descriptions of the conversion properties of RCO can be represented using the block diagram shown in Figure 12.

In the scheme, when describing the arguments of variables, the quantization cycle T_0 is omitted.

The presented block diagram makes it possible to qualitatively evaluate such properties of RCO as controllability and observability, without using the analytical criteria of R. Kalman.

The presented mathematical models of RCO in the nominal mode of its operation allow proceeding to the formation of diagnostic tools taking into account the destabilizing influences on the VES.

4. Diagnostic tools

The diagnostic tools of RCO consist of mathematical models that describe the nominal modes of functional elements and the entire control object, diagnostic models that reflect the relation of indirect signs of diagnosis with direct ones, algorithms for calculating indirect and direct signs of diagnosis, two-digit predicate equations, dichotomous branches and a diagnosis tree.

The diagnostic tools of RCO [15] are developed by sequentially solving the following tasks:

- 1) destabilization detection;
- 2) search for the place of destabilized element;
- 3) establishing the type of destabilizing influence;
- 4) establishing the kind of destabilizing influence;
- 5) formation of the dichotomous diagnostic tree.

4.1. Destabilization detection

The task of detection is to establish the occurrence fact of deviations in the operation of RCO. In order to solve this problem, the reference model of RCO is used that reflects the nominal operating mode in digital form

$$\begin{aligned} \hat{x}[(k+1)T_0] &= A \cdot \hat{x}(kT_0) + b \cdot u(kT_0); \quad x(0) = 0; \\ \hat{u}(k) &= C \cdot \hat{x}(kT_0), \end{aligned} \quad (11)$$

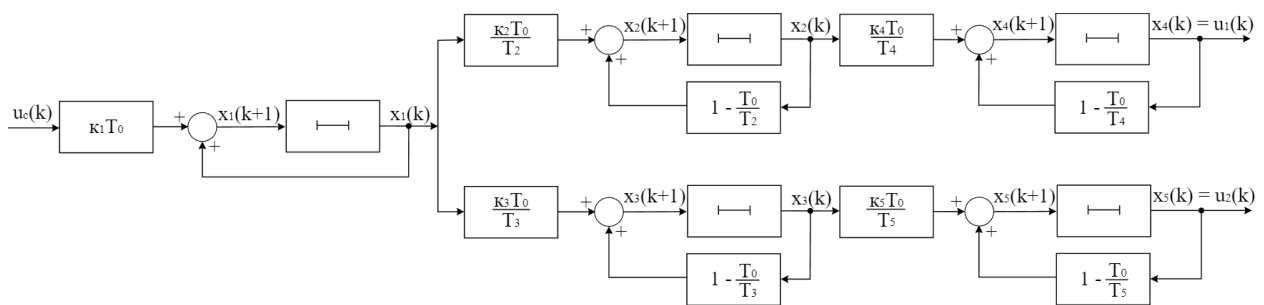


Fig. 12. Block diagram of RCO in the discrete state space

where matrices A , b and C correspond to the matrices of the equation (10), $\hat{x}(kT_0)$ is the reference state vector of RCO, $\hat{u}(kT_0)$ is the reference output vector.

The measurement vector changes $\tilde{u}(kT_0)$ relative to the reference behavior $\hat{u}(kT_0)$ when destabilizing influence appears in RCO. This change can be represented as the following two-digit predicate equation

$$z_0 = S_2 \left\{ \left| \tilde{u}(kT_0) - \hat{u}(kT_0) \right| \geq \delta_0 \right\}; \quad (12)$$

$$k = \overline{k_1, k_2}, p,$$

where S_2 is the two-digit predicate symbol, δ_0 is the deviation tolerance, p is the confidence coefficient.

$$z_0 = \begin{cases} 1, & \text{if } |\Delta u(kT_0)| \geq \delta_0; \\ 0, & \text{if } |\Delta u(kT_0)| < \delta_0, \end{cases} \quad (13)$$

where $\Delta u(kT_0) = \tilde{u}(kT_0) - \hat{u}(kT_0)$, z_0 as true indicates the presence of the fact of destabilization, and z_0 as false indicates its absence.

The confidence coefficient p is used in determining the value of the logical attribute z_0 to eliminate erroneous or noisy discrete deviation values $\Delta u(kT_0)$, which violate conditions (13).

After establishing the fact of destabilization in the RCO, it is necessary to find in which functional element it appeared.

4.2. Search for the place of destabilization

Searching the place of destabilization is related to finding a faulty functional element of RCO under the assumption that only one destabilizing influence can appear during the diagnosis period. The search problem is solved using reference models only for fragments of RCO and using checkpoints that provide the possibility of an unambiguous search, that is, the diagnosability of places of destabilization. There are five such places in

RCO, and a checkpoint is required to ensure diagnosability via the valve position $\mu(t)$. This is ensured by setting a digital valve position sensor that provides measurements of the variable $x_1(t)$ indicated in Figure 12. Then, in order to establish the violation of the servo operability, it is necessary to compare the difference between the signal from the checkpoint $\tilde{u}_\mu(k+1)$ and the signal from the reference model

$$\hat{u}_\mu(k+1) = \hat{u}_\mu(k) + \kappa_1 T_0 u_c(k). \quad (14)$$

with a deviation tolerance δ_1 and process according to the two-digit predicate equation

$$z_1 = S_2 \left\{ \left| \Delta u_\mu(k+1) \right| \geq \delta_1 \right\}; \quad (15)$$

$$k = \overline{k_2, k_3}, p,$$

where $\Delta u_\mu(k+1) = \tilde{u}_\mu(k+1) - \hat{u}_\mu(k+1)$, then

$$z_1 = \begin{cases} 1, & \text{if } \left| \Delta u_\mu(k+1) \right| \geq \delta_1; \\ 0, & \text{if } \left| \Delta u_\mu(k+1) \right| < \delta_1, \end{cases} \quad (16)$$

if z_1 is true, then destabilization has occurred in the servo, and if z_1 is false, then additional checks must be carried out.

In order to search for destabilization in the VES and in temperature sensors, the reference model (11) is used. In this case, two-digit predicate equations are

formed using the components of the measurement vector $u(k)$. So, for the first sensor

$$z_2 = S_2 \left\{ \left| \tilde{u}_1(k) - \hat{u}_1(k) \right| \geq \delta_2 \right\}; \quad (17)$$

$$k = \overline{k_3, k_4}, p$$

and for the second sensor

$$z_3 = S_2 \left\{ \left| \tilde{u}_2(k) - \hat{u}_2(k) \right| \geq \delta_3 \right\}; \quad (18)$$

$$k = \overline{k_3, k_4}, p.$$

Then, if z_2 and z_3 are true, then the destabilization is in the VES, and if z_2 is true and z_3 is false, then this indicates the destabilization of the first sensor, z_2 is false and z_3 is true, then it indicates the destabilization of the second sensor.

A fragment of the dichotomous search tree for the place of destabilization is formed and shown in Figure 13 with the help of logical signs $z_i, i = \overline{0, 3}$.

In case z_0 is true and z_1, z_2, z_3 are false, the scenario is presented when there is destabilization in RCO, but no place has been found. The destabilization detection in this case may be incorrect and therefore it is necessary to return to the destabilization re-detection procedure according to equation (12) appeared.

The next step required to complete the formation of diagnostic tool and expand the dichotomous tree is the establishing the type and kind of destabilization.

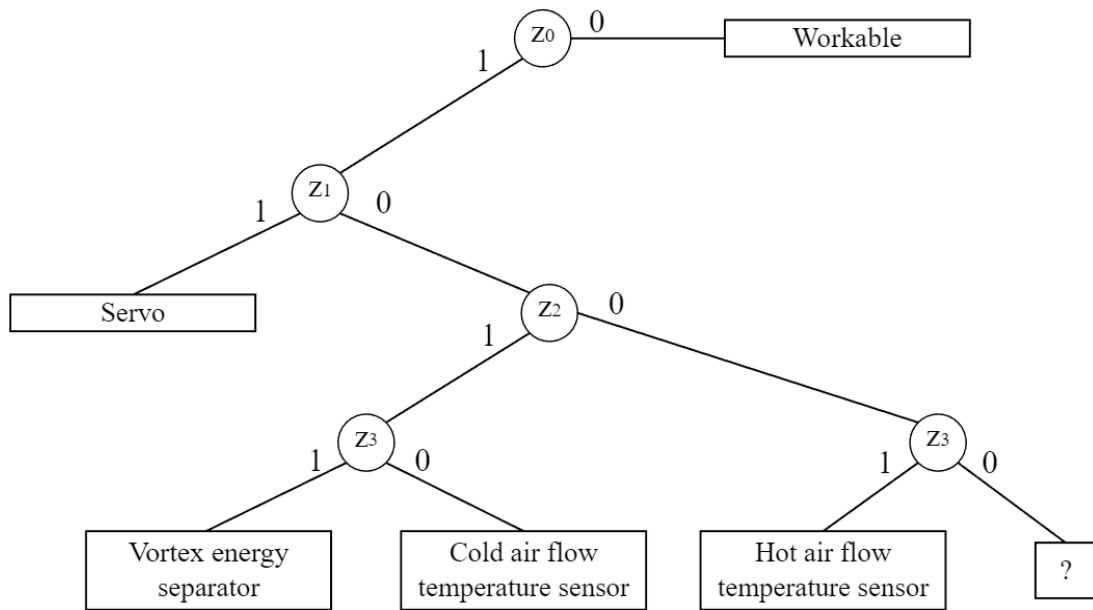


Fig. 13. Fragment of the dichotomous tree

4.3. Destabilization type detection

The destabilizing influences of the servo led to a decrease in the coefficient κ_1 and to the appearance of a zero-drift x_{10} . Therefore, in the process of diagnosing, it is necessary to establish what type of destabilization occurred in the servo. Based on the assumption of a one-time destabilizing influence, which means the impossibility of simultaneously reducing the coefficient and zero-drift, as well as the quasi-stationarity of direct signs of destabilization type in the servo. The argument of the two-digit predicate equation is formed on the basis of the corresponding functional diagnostic models. In order to do this, it is necessary to choose one of two functional diagnostic models that reflect the relation of indirect signs of destabilization with direct signs of types. The direct signs of types are the deviation of the coefficient $\Delta\kappa_1$ and the zero-drift x_{10} . The functional diagnostic model for zero-drift is simpler in structure, obtained by subtracting the equation of the reference model from the servo equation with drift

$$\Delta u_\mu(k+1) = \Delta u_\mu(k) + u_{\mu 0}, \quad (19)$$

where $\Delta u_\mu(k)$ is the deviation of the valve position sensor output signal, $u_{\mu 0}$ is the zero-drift of servo measured by the position sensor. Zero-drift for two dimensions

$$u_{\mu 0} = \Delta u_\mu(k) \quad (20)$$

and for the next two measurements

$$u_{\mu 0} = \Delta u_\mu(k+1). \quad (21)$$

Since the zero-drift does not change over the diagnosing interval due to the assumption of quasi-stationarity, then by equating the right-hand sides of the equations the argument for two-digit predicate equation is formed in the following form

$$|\Delta u_\mu(k+1) - \Delta u_\mu(k)| \leq \delta_{11}, \quad (22)$$

where δ_{11} is the tolerance of zero-drift deviation.

Then the two-digit predicate equation for determining the type of destabilization in the servo is

$$z_{11} = S_2 \left\{ \left| \Delta u_\mu(k+1) - \Delta u_\mu(k) \right| \geq \delta_{11} \right\}; \quad (23)$$

$$k = \overline{k_4, k_5}, \quad p.$$

If z_{11} is false, then this means that there is a zero-drift $u_{\mu 0}$ in the servo. If z_{11} is true type of destabilization is the deviation of the coefficient $\Delta\kappa_1$.

Destabilization in the VES functioning leads to changes in the parameters of mathematical models for both cold and hot air flows. Three types of destabilizations are observed: this is a change in the coefficients κ_2 and κ_3 , time constants T_2 and T_3 , and drifts of operation points θ_{20} and θ_{30} . These types of destabilizations can be established using models of one of the channels.

Let us consider the cold air flow channel during destabilization leading to a change in the coefficient $\tilde{\kappa}_2$. Then the equation of perturbed motion

$$\tilde{x}_2(k+1) = \frac{T_0}{T_2} \tilde{\kappa}_2 x_1(k) + \frac{T_2 - T_0}{T_2} \tilde{x}_2(k) \quad (24)$$

and reference model equation

$$\hat{x}_2(k+1) = \frac{T_0}{T_2} \kappa_2 x_1(k) + \frac{T_2 - T_0}{T_2} \hat{x}_2(k) \quad (25)$$

make it possible to form a functional diagnostic model

$$\Delta x_2(k+1) = \frac{T_0}{T_2} \Delta\kappa_2 x_1(k) + \frac{T_2 - T_0}{T_2} \Delta x_2(k). \quad (26)$$

The discrete signal $\tilde{x}_2(k)$ is calculated using the equation relating $x_3(k) = u_1(k)$ and $x_3(k)$ in the system of finite difference equation (9).

The direct diagnostic sign of the diagnostic type of destabilization from equation (26) is as follows

$$\Delta\kappa_2 = \frac{T_2 \Delta x_2(k+1)}{T_0 x_1(k)} - \frac{(T_2 - T_0) \Delta x_2(k)}{T_0 x_1(k)}. \quad (27)$$

The condition of quasi-stationarity of the sign allows to form the following equality

$$\frac{T_2 \Delta x_2(k+1) - (T_2 - T_0) \Delta x_2(k)}{x_1(k)} = \frac{T_2 \Delta x_2(k+2) - (T_2 - T_0) \Delta x_2(k+1)}{x_1(k+1)} \quad (28)$$

which can be converted to

$$\left[T_2 \Delta x_2(k+1) - (T_2 - T_0) \Delta x_2(k) \right] \cdot x_1(k+1) - \left[T_2 \Delta x_2(k+2) - (T_2 - T_0) \Delta x_2(k+1) \right] \cdot x_1(k) = \gamma_{31}(k+2), \quad (29)$$

then

$$z_{31} = S_2 \left\{ \left| \gamma_{31}(k+2) \right| \leq \delta_{31} \right\}; \quad (30)$$

$$k = \overline{k_4, k_5}, p.$$

If z_{31} is false, then the destabilization is caused by a change in the coefficient $\Delta\kappa_2$, if z_{31} is true the destabilization is caused by the types ΔT_2 and θ_{20} . In order to establish the types of destabilizations of the VES associated with a change in inertial properties is ΔT_2 sign and drift of operation point is θ_{20} sign, the functional diagnostic model for drift can be used

$$\Delta x_2(k+1) = \left(1 - \frac{T_0}{T_2} \right) \Delta x_2(k) + \theta_{20}, \quad (31)$$

which reflects the connection of the direct sign of the destabilization type θ_{20} with the indirect sign $\Delta x_2(k)$. Then the direct sign of destabilization is defined as

$$\theta_{20} = \Delta x_2(k). \quad (32)$$

The value of the sign does not change significantly over the diagnosing interval, so the following equation is

$$\theta_{20} = \Delta x_2(k+1). \quad (33)$$

The following variable can be obtained to form the argument of the two-digit predicate equation by equating equations (32) and (33) and transforming them

$$\left| \Delta x_2(k+1) - \Delta x_2(k) \right| \leq \delta_{32}, \quad (34)$$

then

$$z_{32} = S_2 \left\{ \left| \Delta x_2(k+1) - \Delta x_2(k) \right| \leq \delta_{32} \right\}; \quad (35)$$

$$k = \overline{k_4, k_5}, p.$$

If z_{32} is false the drift of operation point is present. If z_{32} is true the change in the inertial properties of the VES exists.

The destabilization of the cold air sensor operability can be reduced to three types: the decrease in the coefficient by $\Delta\kappa_4$, the increase in the time constant ΔT_4 , and the zero-drift u_{10} .

It is necessary to use the following appropriate functional diagnostic model to determine the type of destabilization leading to a decrease in the coefficient

$$\Delta x_3(k+1) = \left(1 - \frac{T_0}{T_4} \right) \Delta x_3(k) + \frac{\Delta\kappa_4 T_0}{T_4} x_2(k). \quad (36)$$

The variable $x_2(k)$ corresponds to the temperature of the cold air flow. The temperature of cold air is related to the temperature of hot air by the corresponding functional dependence shown in Figure 2. Therefore, the estimated values $x_2(k)$ can be obtained using the measurement results $u_2(k)$ and the corresponding equations for the second sensor. The value of the direct sign $\Delta\kappa_4$ is determined by the following equation

$$\Delta\kappa_4 = \frac{\Delta x_3(k+1) - \left(1 - \frac{T_0}{T_4} \right) \Delta x_3(k)}{x_2(k)} \cdot \frac{T_4}{T_0}. \quad (37)$$

The equation is also valid for subsequent discrete values

$$\Delta\kappa_4 = \frac{\Delta x_3(k+2) - \left(1 - \frac{T_0}{T_4} \right) \Delta x_3(k+1)}{x_2(k+1)} \cdot \frac{T_4}{T_0}. \quad (38)$$

So, the argument variable for a two-digit predicate can be formed as

$$\gamma_{33}(k+2) = \left[\Delta x_3(k+2) - \left(1 - \frac{T_0}{T_4} \right) \Delta x_3(k+1) \right] \times \quad (39)$$

$$\times x_2(k) - \left[\Delta x_3(k+1) - \left(1 - \frac{T_0}{T_4} \right) \Delta x_3(k) \right] \cdot x_2(k+1),$$

then

$$z_{33} = S_2 \left\{ \left| \gamma_{33}(k+2) \right| \leq \delta_{33} \right\}; \quad (40)$$

$$k = \overline{k_4, k_5}, p.$$

If the modulus of the variable $\gamma_{33}(k+2)$ is less over the entire range of k with the confidence coefficient p , then z_{33} is true, which indicates the presence of the first type of destabilization. If z_{33} is false, both the second ΔT_4 and third u_{10} types of destabilizations are possible.

The functional diagnostic model for the zero-drift can be used in order to unambiguously establish these types of destabilizations

$$\Delta x_3(k+1) = \left(1 - \frac{T_0}{T_4} \right) \Delta x_3(k) + u_{10}. \quad (41)$$

The expression for the direct sign u_{10} is

$$u_{10} = \Delta x_3(k). \quad (42)$$

The value of the sign does not change significantly for other values of variables due to quasi-stationarity, therefore

$$u_{10} = \Delta x_3(k+1). \quad (43)$$

The argument variable can be formed based on two equations above

$$|\Delta x_3(k+1) - \Delta x_3(k)| \leq \delta_{34}, \quad (44)$$

then

$$z_{34} = S_2 \left\{ |\Delta x_3(k+1) - \Delta x_3(k)| \leq \delta_{34} \right\}; \quad (45)$$

$$k = \overline{k_4, k_5}, p.$$

If z_{34} is true the zero-drift u_{10} is present, and if z_{34} is false then there is a change in the inertia ΔT_4 .

In the sensor for measuring the temperature of hot air flow, similar three types of destabilizations are possible: the decrease in the coefficient by $\Delta \kappa_5$, increase in the time constant ΔT_5 , and zero-drift u_{20} .

The first type of destabilization is described by a functional diagnostic model

$$\Delta x_5(k+1) = \left(1 - \frac{T_0}{T_5}\right) \Delta x_5(k) + \frac{\Delta \kappa_5 T_0}{T_5} x_4(k), \quad (46)$$

then

$$\Delta \kappa_5 = \frac{\Delta x_5(k+1) - \left(1 - \frac{T_0}{T_5}\right) \Delta x_5(k)}{x_4(k)} \cdot \frac{T_5}{T_0}. \quad (47)$$

The variable $x_4(k)$ is represented by the estimated value through the measurement $u_1(k) = x_3(k)$ of the cold air flow sensor due to the solution of the corresponding equation and the functional connection of the measurements of the temperature sensors.

Then the corresponding argument variable for a two-digit predicate can be represented as

$$\gamma_{35}(k+2) = \left[\Delta x_5(k+2) - \left(1 - \frac{T_0}{T_5}\right) \Delta x_5(k+1) \right] \times \quad (48)$$

$$\times x_4(k) - \left[\Delta x_5(k+1) - \left(1 - \frac{T_0}{T_5}\right) \Delta x_5(k) \right] \cdot x_4(k+1)$$

with the help of which the two-digit predicate equation has the following form

$$z_{35} = S_2 \left\{ |\gamma_{35}(k+2)| \leq \delta_{35} \right\}; \quad (49)$$

$$k = \overline{k_4, k_5}, p.$$

If z_{35} is true there is a first type of destabilization, $\Delta \kappa_5$. If z_{35} is false, both the second ΔT_5 and the third u_{20} types of destabilizations are possible in the considered sensor.

The functional diagnostic model for the zero-drift can be used in order to unambiguously establish these types of destabilizations, as in the previous case

$$\Delta x_5(k+1) = \left(1 - \frac{T_0}{T_5}\right) \Delta x_5(k) + u_{20}. \quad (50)$$

The value of the direct sign of destabilization is determined using the following equation

$$u_{20} = \Delta x_5(k), \quad (51)$$

which allows to form the argument variable for a two-digit predicate equation in this form

$$|\Delta x_5(k+1) - \Delta x_5(k)| \leq \delta_{36}, \quad (52)$$

then

$$z_{36} = S_2 \left\{ |\Delta x_5(k+1) - \Delta x_5(k)| \leq \delta_{36} \right\}; \quad (53)$$

$$k = \overline{k_4, k_5}, p.$$

If z_{36} is true the zero-drift u_{20} is present, and if z_{36} is false so there is a change in the inertia ΔT_5 .

4.4. Determination of the kind of destabilization

The need to solve this problem is associated with various possibilities for recovering the operability of RCO. Destabilizing influences can be of such magnitude that they can be compensated by various means of adjustment. At large values, parrying is performed by means of reconfiguration of algorithms and equipment. Therefore, for each of the previously considered types of destabilizations, two kinds of destabilizing influences will be considered: compensated and uncompensated.

For the servo, if z_{11} is true the type of destabilization $\Delta \kappa_1$ is present. The value of the direct sign is required to determine a specific kind of destabilizing

influence. In this case, this is an estimate of the current value $\Delta\kappa_1(k)$, which is calculated every cycle using the following equation

$$\Delta\kappa_1(k) = \frac{\Delta u_\mu(k+1) - \Delta u_\mu(k)}{T_0 u_c(k)}. \quad (54)$$

The estimated value of the change in the gain of servo can be obtained using the arithmetic average

$$\Delta\hat{\kappa}_1 = \frac{1}{m} \cdot \sum_{i=1}^m \Delta\kappa_1(i). \quad (55)$$

The boundary value $\Delta\bar{\kappa}_1$ can be used to separate two kinds, then via this two-digit predicate equation

$$z_{111} = S_2 \{ \Delta\bar{\kappa}_1 \leq \Delta\hat{\kappa}_1 \} \quad (56)$$

it is possible to diagnose a specific kind of destabilizing influence. If z_{111} is false, then this is the compensated kind d_1 . If z_{111} is true, then this is the uncompensated kind d_2 .

It is necessary to obtain its estimated value using per-tick results to determine the kind of zero-drift of the servo

$$u_{\mu 0}(k) = \Delta u_\mu(k) \quad (57)$$

according to the formula of averaging

$$\hat{u}_{\mu 0} = \frac{1}{m} \cdot \sum_{i=1}^m u_{\mu 0}(i). \quad (58)$$

Then using the two-digit predicate equation

$$z_{110} = S_2 \{ \bar{u}_{\mu 0} \leq \hat{u}_{\mu 0} \}, \quad (59)$$

a specific kind of drift is determined. If z_{110} is false, then this is the compensated kind d_3 . If z_{110} is true, then this is the uncompensated kind d_4 .

Analytical ratios for determining the kinds of change in the coefficient of VES

$$\Delta\kappa_2(k) = \frac{T_2 \Delta x_2(k+1) - (T_2 + T_0) \Delta x_2(k)}{T_0 x_1(k)}; \quad (60)$$

$$\Delta\hat{\kappa}_2 = \frac{1}{m} \cdot \sum_{i=1}^m \Delta\kappa_2(i); \quad (61)$$

$$z_{310} = S_2 \{ \Delta\bar{\kappa}_2 \leq \Delta\hat{\kappa}_2 \}. \quad (62)$$

If z_{310} is false, then this is a compensated kind of change in the coefficient d_5 . If z_{310} is true, then this is its uncompensated kind d_6 .

Ratio for determining the kinds of changes in the inertial properties of VES is

$$\Delta T_2(k) = \frac{T_2^2 \Delta x_2(k+1)}{T_0 [\hat{x}_2(k) - \kappa_2 x_1(k)]}; \quad (63)$$

$$\Delta\hat{T}_2 = \frac{1}{m} \cdot \sum_{i=1}^m \Delta T_2(i); \quad (64)$$

$$z_{321} = S_2 \{ \Delta\bar{T}_2 \leq \Delta\hat{T}_2 \} \quad (65)$$

respectively.

If z_{321} is false, then this is a compensated kinds of change in the coefficient d_7 . If z_{321} is true, then this is its uncompensated kind d_8 .

Ratio for determining the kinds of the drift of operation point of the VES is

$$\Delta\theta_{20}(k) = \Delta x_2(k); \quad (66)$$

$$\Delta\hat{\theta}_{20} = \frac{1}{m} \cdot \sum_{i=1}^m \Delta\theta_{20}(i); \quad (67)$$

$$z_{320} = S_2 \{ \Delta\bar{\theta}_{20} \leq \Delta\hat{\theta}_{20} \}. \quad (68)$$

If z_{320} is false, then this is a compensated kind of the drift of operation point d_9 . If z_{320} is true, then this is its uncompensated kind d_{10} .

Next, the main analytical relations will be considered for diagnosing the kinds of destabilizing influence of the cold air flow sensor.

Ratio for determining the type of change in the coefficient is

$$\Delta\kappa_4(k) = \frac{\Delta x_3(k+1) - \left(1 - \frac{T_0}{T_4}\right) \Delta x_3(k)}{x_2(k)} \cdot \frac{T_4}{T_0}; \quad (69)$$

$$\Delta\hat{\kappa}_4 = \frac{1}{m} \cdot \sum_{i=1}^m \Delta\kappa_4(i); \quad (70)$$

$$z_{331} = S_2 \{ \Delta\bar{\kappa}_4 \leq \Delta\hat{\kappa}_4 \}. \quad (71)$$

If z_{331} is false, then this is a compensated kind of change in the coefficient d_{11} . If z_{331} is true, then this is its uncompensated kind d_{12} .

Ratio for determining the kind of inertia change is

$$\Delta T_4(k) = \frac{\Delta x_3(k+1) - \left(1 - \frac{T_0}{T_4}\right) \Delta x_3(k)}{\tilde{x}_3(k) - \kappa_4 x_2(k)} \cdot \frac{T_4^2}{T_0}; \quad (72)$$

$$\Delta \hat{T}_4 = \frac{1}{m} \cdot \sum_{i=1}^m \Delta T_4(i); \quad (73)$$

$$z_{340} = S_2 \left\{ \Delta \bar{T}_4 \leq \Delta \hat{T}_4 \right\}. \quad (74)$$

If z_{340} is false, then this is a compensated kind of change in inertia d_{13} . If z_{340} is true, then this is its uncompensated kind d_{14} .

Ratio for determining the kind of the drift of operation point is

$$u_{10}(k) = \Delta x_3(k); \quad (75)$$

$$\hat{u}_{10} = \frac{1}{m} \cdot \sum_{i=1}^m u_{10}(i); \quad (76)$$

$$z_{341} = S_2 \left\{ \bar{u}_{10} \leq \hat{u}_{10} \right\}. \quad (77)$$

If z_{341} is false, then this is a compensated kind of the drift of operation point d_{15} . If z_{341} is true, then this is its uncompensated kind d_{16} .

Similarly, the main analytical relations are determined for diagnosing the kinds of destabilizing influences of the hot air flow sensor.

Ratio for determining the kind of change in the coefficient is

$$\Delta \kappa_5(k) = \frac{\Delta x_5(k+1) - \left(1 - \frac{T_0}{T_5}\right) \Delta x_5(k)}{x_4(k)} \cdot \frac{T_5^2}{T_0}; \quad (78)$$

$$\Delta \hat{\kappa}_5 = \frac{1}{m} \cdot \sum_{i=1}^m \Delta \kappa_5(i); \quad (79)$$

$$z_{351} = S_2 \left\{ \Delta \bar{\kappa}_5 \leq \Delta \hat{\kappa}_5 \right\}. \quad (80)$$

If z_{351} is false, then this is a compensated kind of change in the coefficient d_{17} . If z_{351} is true, then this is its uncompensated kind d_{18} .

Ratio for determining the kind of inertial change is

$$\Delta T_5(k) = \frac{\Delta x_5(k+1) - \left(1 - \frac{T_0}{T_5}\right) \Delta x_5(k)}{\tilde{x}_5(k) - \kappa_5 x_4(k)} \cdot \frac{T_5^2}{T_0}; \quad (81)$$

$$\Delta \hat{T}_5 = \frac{1}{m} \cdot \sum_{i=1}^m \Delta T_5(i); \quad (82)$$

$$z_{360} = S_2 \left\{ \Delta \bar{T}_5 \leq \Delta \hat{T}_5 \right\}. \quad (83)$$

If z_{360} is false, then this is a compensated kind of change in inertia d_{19} . If z_{360} is true, then this is its uncompensated form d_{20} .

Ratio for determining the kind of the drift of operation point is

$$u_{20}(k) = \Delta x_5(k); \quad (84)$$

$$\hat{u}_{20} = \frac{1}{m} \cdot \sum_{i=1}^m u_{20}(i); \quad (85)$$

$$z_{361} = S_2 \left\{ \bar{u}_{20} \leq \hat{u}_{20} \right\}. \quad (86)$$

If z_{361} is false, then this is a compensated kind of the drift of operation point d_{21} . If z_{361} is true, then this is its uncompensated kind d_{22} .

4.5. Formation of the dichotomous diagnostic tree

A concept of a state transition diagram (STD) was taken as the basis for constructing the dichotomous tree. STD is used to determine functional safety indicators of a fault-tolerant safety-critical system. As STD method is based on, so this research follows the generalized structure of the state vector with a representation of each functional element of RCO, that allows to classify inoperable states. For STD it is necessary to correctly separate all possible inoperable conditions. Such groups of destabilizations are compensated (may be parried) and uncompensated (reconfiguration, manual intervention) kinds. Thus, the determination of the critical state of system is ensured, in which the value of the sub-predicate expression exceeds the corresponding specified boundary value – the kind of destabilization is uniquely determined [16].

With the help of two-digit dichotomous equations, solutions are obtained in the form of logical variables, which are signs of diagnosing the functional state of RCO. It is possible to systematize them by means of the dichotomous tree shown in Figure 14 using the logical bond of these signs.

Consider the process of forming a deep analysis on a specific example. Let destabilization occur in RCO caused by a change in the time constant of the VES by ΔT_2 exceeding the boundary value, in other words, a destabilization of the kind d_8 occurs.

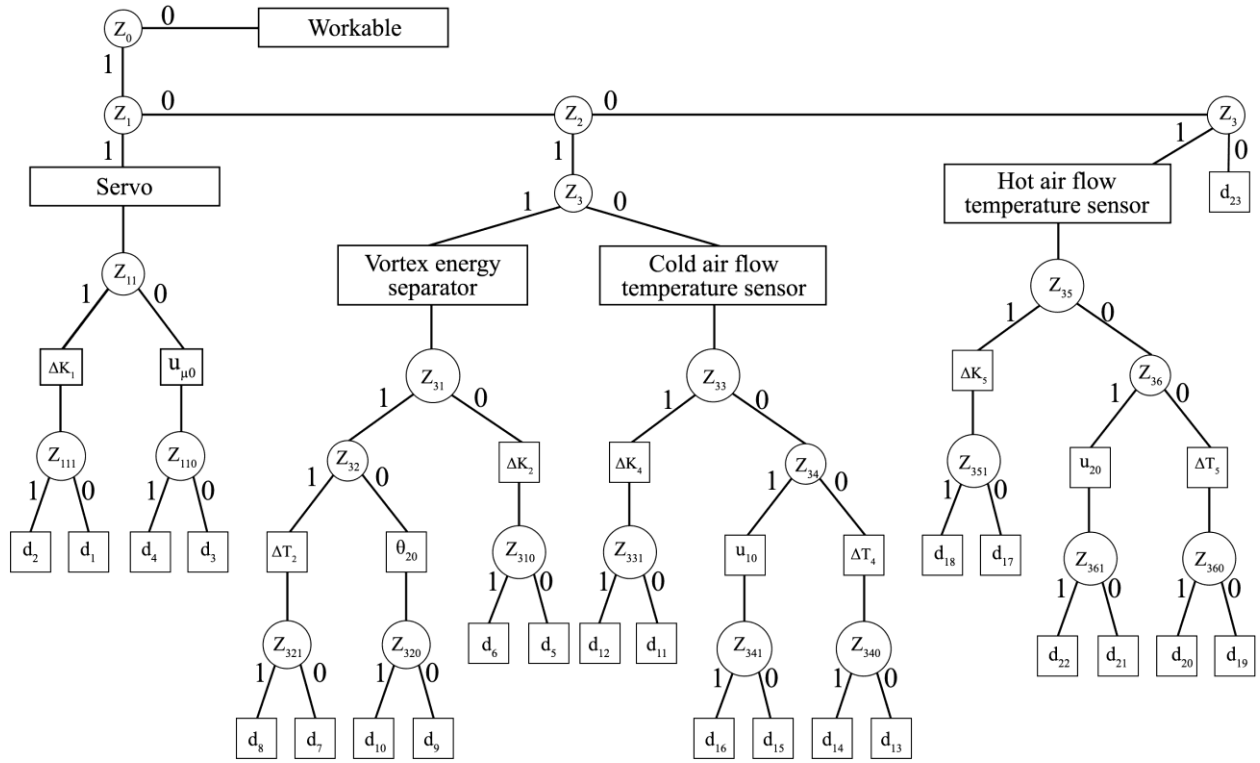


Fig. 14. Dichotomous diagnosis tree

The detection procedure using the predicate equation (12) generates z_0 as true, indicating the inoperability of RCO. Further, using the predicate equation (15), it is established that the servo is operational, since z_1 is false, and the inoperability of RCO is caused by its other functional elements. The predicate equations (17) and (18) says that z_2 and z_3 are true, that indicates the inoperability of VES as a functional element of RCO. Further, from the three possible types of destabilizations, using the solution of predicate equations (30), (35) and (69), it is determined that z_{321} is false, that is, the compensated kind of change in the inertia of VES d_7 .

Similarly, it is possible to analyze the logical relations of the signs involved in the formation of the diagnosis of RCO when each of the 23 kinds of destabilizing influences appears in its functioning.

The dichotomous tree is, in fact, a production knowledge base of emergency situations in the operation of RCO and a logical structure for the relation of this knowledge to form a complete diagnosis of the causes of a malfunction in real time during transients.

5. Recovering tools

After receiving a complete diagnosis of the causes for a malfunction of RCO, it is required to proceed to the following rational control procedures related to the provision of recovery. The recovering tools include redundant, backup funds and algorithms for their flexible

use in accordance with the diagnosis in order to ensure an acceptable level of recovery of RCO. Recovering tools depend both on the type of the functional element of RCO, and on the kinds of its destabilizing influences, as well as on the means of recovery the operability. It is proposed to consider the features of recovering tools for each type of the functional element of RCO.

The considered recovering tool structured by making the following assumptions [17]:

- ACS is considered to be in good working condition in initial state;
- recovery facility is available for each compensated kind of destabilization;
- destabilizing effect is a one-time event, so
- after recovery the functional element is considered to be as good as new;
- recovery rate should not exceed transient time.

5.1. Servo operability recovery

Four kinds of destabilizing actions $d_1 \div d_4$ are diagnosed in the servo. The compensated kind of change in the coefficient ΔK_1 can be carried via the signal adjustment. The value of this adjustment is determined from the equation of the functional diagnostic model

$$\Delta x_1(k+1) = \Delta x_1(k) + \Delta K_1 T_0 u_c(k). \quad (87)$$

It is required to form such an additional control signal at the input of the servo in order to compensate for the resulting deviation $\Delta\kappa_1 T_0 u_c(k)$.

To do that, there is a need to obtain the following equation

$$\tilde{\kappa}_1 T_0 [u_c(k) + u_c'(k)] = \kappa_1 T_0 u_c(k), \quad (88)$$

where $u_c'(k)$ is the adjustment signal.

The solution of this equation with respect to the adjustment signal

$$u_c'(k) = \frac{(\kappa_1 - \tilde{\kappa}_1)}{\tilde{\kappa}_1} \cdot u_c(k) = \frac{\Delta\kappa_1}{\kappa_1 - \Delta\kappa_1} \cdot u_c(k). \quad (89)$$

It is necessary to use $\Delta\kappa_1$ to implement the adjustment signal, then the equation

$$u_c'(k) = \frac{\Delta\hat{\kappa}_1}{\kappa_1 - \Delta\hat{\kappa}_1} \cdot u_c(k) \quad (90)$$

will provide compensation for the current deviation $\Delta\kappa_1$ and recover the servo.

The adjustment signal is used to recover the operability in case of compensated type of destabilizing influence d_4 , associated with the appearance of a zero-drift of the servo. The value of the signal adjustment is determined from the equation of the perturbed motion of the servo

$$\tilde{x}_1(k+1) = \tilde{x}_1(k) + \kappa_1 T_0 u_c(k) + T_0 u_{\mu 0}. \quad (91)$$

Based on the zero-drift compensation condition, the following equality can be formed

$$\kappa_1 T_0 [u_c(k) + u_c'(k)] + T_0 u_{\mu 0} = \kappa_1 T_0 u_c(k) \quad (92)$$

from which the adjustment signal is determined as

$$u_c'(k) = -\frac{\hat{u}_{\mu 0}}{\kappa_1}. \quad (93)$$

When uncompensated kinds of destabilizing influences d_2 and d_3 appear in the servo, an additional backup electric motor must be used to recover the operability, which can go both in cold and hot standby. In this case, using the hardware reconfiguration tool, the faulty electric motor is switched off and the backup option is put into operation, that ensures the servo recovery.

5.2. VES operability recovery

The violation of operability of the VES is due to six kinds of destabilizing influences $d_5 \div d_{10}$. Consid-

er the recovery procedures for each kind of compensated destabilizing influences.

The functional diagnostic model for the type of destabilization caused by a change in the coefficient $\Delta\kappa_3$ is described by the following equation

$$\Delta x_2(k+1) = \frac{T_0 \Delta\kappa_2}{T_2} x_1(k) + \frac{T_2 - T_0}{T_2} \Delta x_2(k). \quad (94)$$

In order to compensate for the first component of the right part of the equation, it is necessary to form such an additional control signal $u_c'(k)$ that the third term $-\frac{T_0 \Delta\hat{\kappa}_2}{T_2} x_1(k)$ appears.

If the additional control signal is

$$u_c'(k+2) = \frac{\Delta\hat{\kappa}_2}{T_2 \kappa_1} [x_1(k+1) - x_1(k)], \quad (95)$$

then the change in the coefficient of the VES will be compensated by switching to another operation point.

Compensation for the kind d_7 of the destabilizing influence associated with an increase in the inertia of the VES by the value of ΔT_2 can be made by reconfiguring the control algorithm. Using a functional diagnostic model

$$\Delta x_2(k+1) = \frac{T_0 \Delta T_2}{T_2^2} \Delta x_2(k) - \frac{\kappa_2 T_0 \Delta T_2}{T_2^2} x_1(k), \quad (96)$$

the following algorithm is formed

$$\hat{x}_1(k+2) = \frac{T_2^2}{\kappa_2 T_0 \Delta \hat{T}_2} \left[\frac{T_0 \Delta \hat{T}_2}{T_2^2} \Delta x_2(k) - \Delta x_2(k+1) \right]. \quad (97)$$

It is necessary to use the measurable variable $x_2(k)$ indicated in Figure 12 for the practical implementation of this algorithm, applying the equations of relation with the variable $x_2(k)$, which is not measurable, and then the additional signal will be calculated through the deviations $\Delta x_3(k)$.

This additional signal is formed with the help of

$$u_c'(k+4) = \frac{x_1'(k+3) - x_1'(k+2)}{\kappa_1 T_0}. \quad (98)$$

It provides forced control of the VES in order to compensate for the deceleration of transient process.

The compensation of the drift of operation point, kind d_9 , can be done with an adjustment signal. Based on the equation of the functional diagnostic model (31), to compensate the drift of operation point by the value θ_{20} , it is required to change the signal $x_2(k)$ at the input of the VES by this value. This change corre-

sponds to the situation in the servo at d_4 . Then, using the structure of equation (93), it can be determined that the additional signal will be

$$u_c'(k) = -\frac{\hat{\theta}_{20}}{\kappa_1 T_0}. \quad (99)$$

Such an additional control signal will make it possible to compensate the drift of operation point of the VES caused by the destabilization kind d_4 .

Uncompensated kinds of destabilizing influences d_5 , d_8 and d_{10} cannot be parried by any instrumental means in such a way as to recover the full operability of the VES. Therefore, if the conditions of operation allow the use the VES with such changes in parameters, then further operation is carried out, which is much better than the complete shutdown of the vortex energy separation process to stabilize temperature modes.

5.3. Temperature sensors operability recovery

The change in the operability of the cold air flow sensor occurs due to six kinds of destabilizing influences $d_{11} \div d_{16}$. In order to recover the measurements of the inoperative cold air flow sensor, a number of means can be used: signal adjustment of deviations $\Delta\kappa_4$ and u_{10} , reconfiguration of the control algorithm when changing ΔT_4 , as well as measurements of the hot air flow sensor and measurements recovery by using a reference model.

The recovery of operability with the help of signal adjustment and reconfiguration of control algorithms have already been considered earlier in this paper. Therefore, the following will describe the process of recovering the measurements of the inoperative cold air flow temperature sensor using the measurements of the hot air flow temperature sensor. Sensor measurements are interconnected by

$$x_3(k) = x_5(k) - \theta(\mu), \quad (100)$$

where $\theta(\mu)$ is the difference in temperature measuring depending on the valve position μ indicated in Figure 2. Therefore, for all possible kinds of destabilizing influences, instead of incorrect measurements of the cold air flow temperature sensor, estimated measurements could be used

$$\hat{x}_3(k) = x_5(k) - \theta(x_1(k)), \quad (101)$$

where the variable $x_1(k)$ reflects the valve position.

Measurements of the inoperative cold air flow temperature sensor can be replaced by estimated measurements obtained using the reference model

$$\begin{cases} \hat{x}_2(k+1) = \left(1 - \frac{T_0}{T_2}\right) \hat{x}_2(k) + \frac{\kappa_2 T_0}{T_2} \cdot \frac{u_\mu(k)}{\kappa_1}; \\ \hat{x}_3(k+1) = \left(1 - \frac{T_0}{T_4}\right) \hat{x}_3(k) + \frac{\kappa_4 T_0}{T_4} \cdot \hat{x}_2(k). \end{cases} \quad (102)$$

The variable $\hat{x}_3(k)$ is an estimated measurement of the cold air flow temperature sensor, which corresponds to the VES nominal operation mode and the hot air flow temperature sensor.

The recovery of the inoperable hot air flow temperature sensor measurements can be done in the same way. When using the cold air flow sensor measurements, the estimated measurements will be generated by means of

$$\hat{x}_5(k) = x_3(k) + \theta(x_1(k)). \quad (103)$$

Estimated measurements using the reference model are obtained by solving the system of equations

$$\begin{cases} \hat{x}_2(k+1) = \left(1 - \frac{T_0}{T_2}\right) \hat{x}_2(k) + \frac{\kappa_2 T_0}{T_2} \cdot \frac{u_\mu(k)}{\kappa_1}; \\ \hat{x}_3(k+1) = \left(1 - \frac{T_0}{T_4}\right) \hat{x}_3(k) + \frac{\kappa_4 T_0}{T_4} \cdot \hat{x}_2(k). \end{cases} \quad (104)$$

The variable $\hat{x}_5(k)$ is the estimated measurement of the hot air flow temperature sensor, which corresponds to the VES nominal operation mode and the cold air flow temperature sensor.

The presented algorithms for recovering the operability of RCO do not content the whole variety of possible way of the destabilizing influences kinds responding. An important point in the choice of means is the assumption that the worst contingency is possible in the future. Therefore, in the excess means reserve, there should be such ones that will allow it to be neutralized any destabilization ensuring the autonomous functioning of the vortex energy separation process.

Conclusions

The purpose of the article is to apply the rational control of VES under conditions of destabilizing influences. The use of rational control requires the formation of ACO, which includes the servo, VES and temperature sensors of cold and hot air flows. The processing of the experimental data made it possible to form linearized mathematical models in form of transfer functions and state space equations for the nominal operating mode, i.e., in the absence of destabilizing influences.

The destabilizing influences on the functional elements of ACO make it possible to form a number of diagnostic models that analytically reflect the relation between indirect and direct signs of diagnosis. The problems of detecting destabilization, finding its place, establishing the type and determining the kind of destabilizing influences were solved with the help of those diagnostic models. Thus, it is possible to form a knowledge base and a structure of inference about the causes of destabilization in form of a dichotomous tree. Algorithms for the rehabilitation of the operable state of VES are formed for each kind of destabilization.

As a result of solving the research problems, an approach was proposed to the development of models and algorithms for the rational control of VES under conditions of destabilizing influences. The proposed approach makes it possible to control the operable state of VES and to ensure high-quality control of the output air flow temperature.

In the future, it is necessary to expand the class of diagnostic models, taking into account the physics of processes occurring in the control system, the nonlinear and non-stationary properties of real objects. In addition, building up the diagnostic production knowledge base will allow the RCS to process a greater number of destabilizing influences. The combination of the model and the knowledge base can be applied to a real control system to detect faults early, decide on the acceptability of errors, and then fend off these faults without resorting to letup the control system operation. The non-linear characteristics of VES can be taken into account via the interval parameters of its linearized models. It should help to cover the entire functionality of VES as a united variegated object.

Contribution of authors: purpose and tasks formulation of the rational control, original draft development of diagnostic models – **Anatoliy Kulik**; concept and methodology development of the research – **Kostiantyn Dergachov**; experimental characteristics of the vortex energy separator, mathematical models of nominal operation mode, text review – **Sergiy Pasichnik**; review and analysis of references, application of the rational control concept to the vortex energy separator, text writing and editing – **Dmytro Sokol**.

All the authors have read and agreed to the published version of the manuscript.

References (GOST 7.1:2006)

1. Ranque, G. J. *Experiments on Expansion in a Vortex with Simultaneous Exhaust of Hot Air and Cold Air* [Text] / G. J. Ranque // *Le Journal de Physique et le Radium*. – 1933. – Vol. 4, no. 6. – P. 112-114.

2. Меркулов, А. П. *Вихревой эффект и его применение в технике* [Текст] / А. П. Меркулов. – М. : Машиностроение, 1969. – 185 с.

3. Kulik, A. S. *Investigation of Stationary Processes in Vortex Energy Separator Through Its Computational Fluid Dynamics Model* [Text] / A. S. Kulik, S. N. Pasichnik, D. V. Sokol // *Mathematical Modeling and Simulation of Systems : Selected Papers of 16th International Scientific-practical Conference, MODS, Chernihiv, June 28 – July 01, 2021*. – P. 105-114. DOI: 10.1007/978-3-030-89902-8_8.

4. Халатов, А. А. *Теория и практика закрученных потоков* [Текст] / А. А. Халатов. – Киев : Наукова думка, 1989. – 192 с.

5. Кулік, А. С. *Апаратно-програмний комплекс для дослідження вихрового ефекту* [Текст] / А. С. Кулік, В. Г. Джулгаков, С. М. Пасичник // *Вісник ХНТУСГ*. – 2010. – Вип. 102. – С. 85-87.

6. Rafiee, S. E. *Experimental and 3D CFD investigation on energy separation inside a convergent vortex tube air separator* [Text] / S. E. Rafiee, M. M. Sadeghiazad // *Scientia Iranica*. – 2016. – Vol. 23, iss. 4. – P. 1753-1766. DOI: 10.24200/sci.2016.3923.

7. Kim, Y. *A Study on the Application Possibility of the Vehicle Air Conditioning System Using Vortex Tube* [Text] / Y. Kim, S. Im, J. Han // *Energies*. – 2020. – Vol. 13, no. 19. – Article No. 5227. DOI: 10.3390/en13195227.

8. Sagar Manmath Swami. *Design and Development of a Cooling System for A Vaccine Container by using Vortex Tube Refrigeration* [Text] / Sagar Manmath Swami, Kunal Y. Bhavsar // *International journal of engineering research & technology (IJERT)*. – 2022. – Vol. 11, no. 7. – P. 169-177. DOI: 10.17577/IJERTV11IS070093.

9. *Modeling and thermal analysis of a solar thermoelectric generator with vortex tube for hybrid vehicle* [Text] / B. E. M. Fotso, R. C. Talawo, M. C. Feudjio Nguetack, M. Fogue // *Case Studies in Thermal Engineering*. – 2019. – Vol. 15. – Article No. 100515. DOI: 10.1016/j.csite.2019.100515.

10. *Integration of vortex tubes in a trigenerative compressed air energy storage system* [Text] / E. Beaugendre, J. Lagrandeur, M. Cheayb, S. Poncet // *Energy Conversion and Management*. – 2021. – Vol. 240. – Article No. 114225. DOI: 10.1016/j.enconman.2021.114225.

11. Bazgir, A. *Numerical investigation of the effects of geometrical parameters on the vortex separation phenomenon inside a Ranque-Hilsch vortex tube used as an air separator in a helicopter's engine* [Text] / A. Bazgir, N. Nabhani // *Aviation*. – 2018. – Vol. 22, no. 1. – P. 13-23. DOI: 10.3846/aviation.2018.2414.

12. *Exploring Various Control Systems and Its Application* [Text] / R. Lakshmanababu, D. Mahesh, I. Arun Pandyan, M. Ramachandran, Kurinjimalar Ramu // *Electrical and Automation Engineering*. – 2022. – Vol. 1, no. 1. – P. 40-46. DOI: 10.46632/ae/1/1/7.

13. Le, Q. D. An Active Fault-Tolerant Control Based on Synchronous Fast Terminal Sliding Mode for a Robot Manipulator [Text] / Q. D. Le, H.-J. Kang // *Actuators*. – 2022. – Vol. 11, no. 7. – Article No. 195. DOI: 10.3390/act11070195.

14. Review of Control Techniques for HVAC Systems—Nonlinearity Approaches Based on Fuzzy Cognitive Maps [Text] / F. Behrooz, N. Mariun, M. Marhaban, M. Mohd Radzi, A. Ramli // *Energies*. – 2018. – Vol. 11, no. 3. – Article No. 495. DOI: 10.3390/en11030495.

15. Diagnostic models of inoperable states of the vortex energy separator device [Text] / A. Kulik, K. Dergachov, S. Pasichnik, D. Sokol // *Авіаційно-космічна техніка і технологія*. – 2022. – No. 3(179). – P. 13-29. DOI: 10.32620/aktt.2022.3.02.

16. Functional safety analysis of safety-critical system using state transition diagram [Text] / L. Ozirkovskyy, B. Volochiy, O. Shkiliuk, M. Zmysnyi, P. Kazan // *Радіоелектронні і комп'ютерні системи*. – 2022. – № 2(102). – P. 145-158. DOI: 10.32620/reks.2020.2.02.

17. Tyagi, S. Stochastic hybrid energy system modelling with component failure and repair [Text] / S. Tyagi, N. Goyal, A. Kumar, M. Ram // *International Journal of System Assurance Engineering and Management*. – 2021. – 11 p. DOI: 10.1007/s13198-021-01129-4.

References (BSI)

1. Ranque, G. J. Experiments on Expansion in a Vortex with Simultaneous Exhaust of Hot Air and Cold Air. *Le Journal de Physique et le Radium*, 1933, vol. 4, no. 6, pp. 112-114.

2. Merkulov, A. P. *Vikhrevoi effekt i ego primeneniye v tekhnike* [Vortex effect and its application in engineering]. Moscow, Mashinostroenie Publ., 1969. 185 p.

3. Kulik, A. S., Pasichnik, S. N., Sokol, D. V. Investigation of Stationary Processes in Vortex Energy Separator Through Its Computational Fluid Dynamics Model. *Mathematical Modeling and Simulation of Systems : Selected Papers of 16th International Scientific-practical Conference, MODS*, Chernihiv, June 28–July 01, 2021, pp. 105-114. DOI: 10.1007/978-3-030-89902-8_8.

4. Khalatov, A. A. *Teoriya i praktika zakruchennykh potokov* [Theory and practice of swirling flows]. Kyiv, Naukova dumka Publ., 1989. 192 p.

5. Kulik, A. S., Dzhulgakov, V. G., Pasichnik, S. N. Aparatno-prohramnyy kompleks dlya doslidzhennya vykhrovoho efektu [Hardware and software complex for investigating the vortex effect]. *Visnyk KhNTUSH – Messenger KhNTUSH*, 2010, no. 102, pp. 85-87.

6. Rafiee, S. E., Sadeghiazad, M. M. Experimental and 3D CFD investigation on energy separation inside a convergent vortex tube air separator. *Scientia Iranica*, 2016, vol. 23, iss. 4, pp. 1753-1766. DOI: 10.24200/sci.2016.3923.

7. Kim, Y., Im, S., Han, J. A Study on the Application Possibility of the Vehicle Air Conditioning System Using Vortex Tube. *Energies*, 2020, vol. 13, no. 19, article no. 5227. DOI: 10.3390/en13195227.

8. Sagar Manmath Swami, Kunal Y. Bhavsar. Design and Development of a Cooling System for A Vaccine Container by using Vortex Tube Refrigeration. *International journal of engineering research & technology (IJERT)*, 2022, vol. 11, no. 7, pp. 169-177. DOI: 10.17577/IJERTV11IS070093.

9. Fotso, B. E. M., Talawo, R. C., Feudjio Nguéfack, M. C., Fogue, M. Modeling and thermal analysis of a solar thermoelectric generator with vortex tube for hybrid vehicle. *Case Studies in Thermal Engineering*, 2019, vol. 15, article no. 100515. DOI: 10.1016/j.csite.2019.100515.

10. Beaugendre, E., Lagrandeur, J., Cheayb, M., Poncet, S. Integration of vortex tubes in a trigenerative compressed air energy storage system. *Energy Conversion and Management*, 2021, vol. 240, article no. 114225. DOI: 10.1016/j.enconman.2021.114225.

11. Bazgir, A., Nabhani, N. Numerical investigation of the effects of geometrical parameters on the vortex separation phenomenon inside a Ranque-Hilsch vortex tube used as an air separator in a helicopter's engine. *Aviation*, 2018, vol. 22, no. 1, pp. 13-23. DOI: 10.3846/aviation.2018.2414.

12. Lakshmanababu, R., Mahesh, D., Arun Pandyan, I., Ramachandran, M., Kurinjimalar Ramu. Exploring Various Control Systems and Its Application. *Electrical and Automation Engineering*, 2022, vol. 1, no. 1, pp. 40-46. DOI: 10.46632/eae/1/1/7.

13. Le, Q. D., Kang, H.-J. An Active Fault-Tolerant Control Based on Synchronous Fast Terminal Sliding Mode for a Robot Manipulator. *Actuators*, 2022, vol. 11, no. 7, article no. 195. DOI: 10.3390/act11070195.

14. Behrooz, F., Mariun, N., Marhaban, M., Mohd Radzi, M., Ramli, A. Review of Control Techniques for HVAC Systems—Nonlinearity Approaches Based on Fuzzy Cognitive Maps. *Energies*, 2018, vol. 11, no. 3, article no. 495. DOI: 10.3390/en11030495.

15. Kulik, A., Dergachov, K., Pasichnik, S., Sokol, D. Diagnostic models of inoperable states of the vortex energy separator device. *Авіаційно-космічна техніка і технологія – Aerospace technic and technology*, 2022, no. 3(179), pp. 13-29. DOI: 10.32620/aktt.2022.3.02.

16. Ozirkovskyy, L., Volochiy, B., Shkiliuk, O., Zmysnyi, M., Kazan, P. Functional safety analysis of safety-critical system using state transition diagram. *Radioelektronni i komp'uterni sistemi – Radioelectronic and computer systems*, 2022, no. 2 (102), pp. 145-158. DOI: 10.32620/reks.2020.2.02.

17. Tyagi, S., Goyal, N., Kumar, A., Ram, M. Stochastic hybrid energy system modelling with component failure and repair. *International Journal of System Assurance Engineering and Management*, 2021. 11 p. DOI: 10.1007/s13198-021-01129-4.

Надійшла до редакції 12.05.2022, розглянута на редколегії 25.08.2022

РАЦІОНАЛЬНЕ УПРАВЛІННЯ ТЕМПЕРАТУРОЮ ВИХРОВОГО ЕНЕРГОРОЗДІЛЬНИКА ПРИ ДЕСТАБІЛІЗУЮЧИХ ВПЛИВАХ

А. С. Кулік, К. Ю. Дергачов, С. М. Пасічник, Д. В. Сокол

Об'єктом дослідження у статті є процес формування раціонального управління температурою вихрового енергороздільника при дестабілізуючих впливах. **Предметом** статті є процес формування дихотомічного дерева за двозначними предикатами діагностичних моделей пристрою вихрового енергороздільника як об'єкта раціонального управління при появі дестабілізуючих впливів, та подальше відновлення його працездатності. **Метою** є розробка аналітичного підходу до формування цифрових алгоритмів раціонального управління температурою холодного і гарячого потоків повітря вихрового раціонального. **Задачі:** вивчити особливості процесу у пристрої вихрового енергороздільника; описати раціональну систему керування пристроєм вихрового енергороздільника; провести аналіз експериментальних характеристик пристрою вихрового енергороздільника; сформувані лінійні математичні моделі номінального режиму роботи вихрового енергороздільника; розробити лінійні діагностичні моделі, що описують непрацездатні стани вихрового енергороздільника як раціонального об'єкта управління; сформувані логічні ознаки діагностування за допомогою діагностичних моделей, розробити алгоритми відновлення працездатності вихрового енергороздільника. Використовуваними **методами** є: передавальні функції, дискретний простір станів, формування продукційних правил, двозначні предикатні рівняння, дихотомічні дерева, діагностика та відновлення працездатності динамічних об'єктів. Отримано такі **результати:** аналіз особливостей процесу вихрового енергоподілу, опис структури та функцій раціональної системи управління, аналіз експериментальних характеристик, побудова математичних моделей, розробка засобів діагностики та відновлення аварійного режиму роботи вихрового енергороздільника як раціонального об'єкта управління при заданому наборі дестабілізуючих впливів. **Висновки.** Наукова новизна полягає у формуванні аналітичного підходу до розробки раціонального управління процесом вихрового енергоподілу повітряного потоку при значній дії різного роду дестабілізуючих впливів.

Ключові слова: вихрова трубка Ранка-Хілша; вихровий енергороздільник; раціональне управління; дестабілізуючі впливи; лінійні математичні моделі; двозначні предикатні рівняння; діагностичне забезпечення; реабілітаційне забезпечення.

Кулік Анатолій Степанович – д-р техн. наук, проф. каф. «Системи управління літальними апаратами», Національний аерокосмічний університет ім. М. Є. Жуковського «Харківський авіаційний інститут», Харків, Україна.

Дергачов Костянтин Юрійович – канд. техн. наук, старш. наук. співроб., зав. каф. «Системи управління літальними апаратами», Національний аерокосмічний університет ім. М. Є. Жуковського «Харківський авіаційний інститут», Харків, Україна.

Пасічник Сергій Миколайович – канд. техн. наук, доц. каф. «Системи управління літальними апаратами», Національний аерокосмічний університет ім. М. Є. Жуковського «Харківський авіаційний інститут», Харків, Україна.

Сокол Дмитро Вадимович – ас. каф. «Системи управління літальними апаратами», Національний аерокосмічний університет ім. М. Є. Жуковського «Харківський авіаційний інститут», Харків, Україна.

Anatoliy Kulik – Doctor of Technical Sciences, Professor of the Department «Control Systems of Aircraft», National Aerospace University «Kharkiv Aviation Institute», Kharkiv, Ukraine, e-mail: anatoly.kulik@gmail.com, ORCID: 0000-0001-8253-8784.

Kostiantyn Dergachov – Candidate of Technical Sciences, senior researcher, Head of the Department «Control Systems of Aircraft», National Aerospace University «Kharkiv Aviation Institute», Kharkiv, Ukraine, e-mail: k.dergachov@khai.edu, ORCID: 0000-0002-6939-3100.

Sergiy Pasichnik – Candidate of Technical Sciences, Associate professor of the Department «Control Systems of Aircraft», National Aerospace University «Kharkiv Aviation Institute», Kharkiv, Ukraine, e-mail: snpasichnik@gmail.com, ORCID: 0000-0001-7016-8835.

Dmytro Sokol – Assistant of the Department «Control Systems of Aircraft» Department, National Aerospace University «Kharkiv Aviation Institute», Kharkiv, Ukraine, e-mail: d.sokol@khai.edu, ORCID: 0000-0003-0847-350X.